scientific reports

Check for updates

OPEN

Cationized extracellular vesicles for gene delivery

Natalia L. Klyachko[1,2]✉, Matthew J. Haney[1,3], Anton V. Lopukhov[2] & Irina M. Le-Deygen[2]

Last decade, extracellular vesicles (EVs) attracted a lot of attention as potent versatile drug delivery vehicles. We reported earlier the development of EV-based delivery systems for therapeutic proteins and small molecule chemotherapeutics. In this work, we first time engineered EVs with multivalent cationic lipids for the delivery of nucleic acids. Stable, small size cationized EVs were loaded with plasmid DNA (*p*DNA), or mRNA, or siRNA. Nucleic acid loaded EVs were efficiently taken up by target cells as demonstrated by confocal microscopy and delivered their cargo to the nuclei in triple negative breast cancer (TNBC) cells and macrophages. Efficient transfection was achieved by engineered cationized EVs formulations of *p*DNA- and mRNA in vitro. Furthermore, siRNA loaded into cationized EVs showed significant knockdown of the reporter gene in Luc-expressing cells. Overall, multivalent cationized EVs represent a promising strategy for gene delivery.

Keywords Cancer, EVs, Gene delivery, Multivalent cationic lipid, Transfection

Gene delivery has remained the focus of numerous studies over several decades. Yet, it remains a challenge because of low stability of nucleic acids in the blood stream, along with their limited permeability across biological barriers. Multiple nanoformulations were developed to accomplish this challenging task. Among them are solid core nanoparticles, polyion complexes, liposomes, etc[1]. Recently, the smart nanocarriers with response to pH changes, reactive oxygen species, glutathione concentration, and presence of several enzymes as well as nanocarriers sensitive to the external stimuli like light and magnetic field are discussed[2]. Stimuli-responsive lipoplexes or polyplexes are considered as most versatile gene-delivery platforms and were widely studied in recent years[3–5]. These vehicles are suitable for variable routes of administration, including systemic, intracranial and intrathecal injections as well as intranasal introduction[6]. Regrettably, these efforts have been met with limited success. The main impediment is the opsonization of drug-loaded nanoparticles in the bloodstream and rapid drug clearance by mononuclear phagocyte system (MPS)[7,8]. To solve this problem, a polyethylene glycol (PEG) corona was introduced to perpetuate a stealth effect. However, along with the decreasing drug uptake by MPS, the PEGylation concurrently reduced the interaction with target cells, thus, decreasing drug transport and its therapeutic efficiency[9–11]. In addition, a rapid immune response to the PEG corona significantly increased clearance of PEGylated drug nanocarriers[12–15]. Finally, the administration of different types of nanoparticles followed by their opsonization was reported to induce chronic autoimmune diseases such as rheumatoid arthritis[16,17]. Clearly, there is an unmet medical need in the area of gene delivery for novel therapeutic approaches. To circumvent this problem, we propose using EVs for systemic administration. EVs have benefits of both synthetic nanocarriers and cell-mediated drug delivery systems, and at the same time, avoid their limitations[18]. Comprised of cellular membranes with multiple adhesive proteins on their surface[19,20], EVs are able to efficiently interact and fuse with membranes of target cells and deliver their cargo[21,22]. Natural protection of exosomes from both complement binding and recognition and phagocytosis by macrophages significantly increases delivery potency[23–25]. For example, it has been demonstrated that EVs loaded siRNA effectively knockdowns targets in mice with 10 times lower dosage[26]. The employment of exosomes for gene delivery is actively explored as emerging strategy of therapy for a number pathological condition including various cancers[27,28].

One of the main problem in cancer therapy is the treatment of triple negative breast cancer (TNBC), where the three most common types of receptors known to fuel most breast cancer growth–estrogen, progesterone, and the HER-2/neu gene– are not present in the cancer tumor[29,30]. In addition, diverse components of the breast cancer microenvironment, such as suppressive immune cells, re-programmed fibroblast cells, altered extracellular matrix (ECM) and certain soluble factors, synergistically impede an effective anti-tumor response and promote

[1]Division of Pharmacoengineering and Molecular Pharmaceutics, UNC Eshelman School of Pharmacy, University of North Carolina at Chapel Hill, Chapel Hill, NC 27599-7362, USA. [2]Deparment of Chemical Enzymology, Faculty of Chemistry, Lomonosov Moscow State University, Moscow, Russia. [3]Center for Nanotechnology in Drug Delivery, Carolina Institute for Nanomedicine, University of North Carolina at Chapel Hill, Chapel Hill, NC, USA. ✉email: nlklyachko@gmail.com; klyachko@ad.unc.edu

breast cancer progression and metastasis[31]. Thus, development of drug formulations for chemotherapy to eliminate TNBC cells, as well as for tumor microenvironment (TME) is of great importance.

We reported earlier the development of various EV-based formulations for therapeutic proteins and small molecule chemotherapeutics[32–39]. Specifically, EV-based formulations of anticancer agents, Doxorubicin and Paclitaxel were developed to treat pulmonary metastases[32,37]. Exosomes were successfully employed for delivery of cytochrome C (cytC), an inducer of apoptosis in cancer cells[40]. Furthermore, EVs loaded with antioxidants such as catalase, or neuronal growth factors, GDNF or BDNF, provided significant neuroprotective effects in in vitro and in vivo models of Parkinson's disease (PD), stroke, and LPS-induces encephalitis[33,34,36]. Of note, EVs derived from autologous macrophages may exert unique biological activity reflective of their origin that allows them to penetrate the biological barriers and migrate rapidly to sites of inflammation and cancer[41]. Herein, we utilized macrophage-derived EVs to develop novel formulations for different nucleic acids (EV-Gene) including *p*DNA, mRNA, and siRNA thought the modification of EVs surface with a cationic lipid (Fig. 1).

The EVs surface is negatively charged that impedes interaction with negatively charged nucleic acids. Therefore, we suggested that to increase loading efficiency, EVs should be cationized. Furthermore, cationic lipids were shown to improve loading of nucleic acids into liposomes[42–45]. The understanding of the role of cationic lipids in the development of lipid-based vehicles for gene delivery is crucial[46]. Yet, just one positive charge of the cationic lipid that binds with negatively charged proteins and/or lipids on EVs surface, may not be sufficient for stable complex with therapeutic genes. Therefore, we propose to use multivalent cationic lipid, MVL5, for EVs membrane modification. We hypothesized that hydrophobic tail of the MVL5 lipid molecule will be easily incorporated into hydrophobic part of lipid bilayer of EVs membranes, and five cationic groups will be available for interactions with not only proteins and/or lipids on the EVs surface, but also with therapeutic genes to deliver. Therapeutic efficacy of EV-based formulations (EV-Genes) was demonstrated in TNBC cells as well as macrophages as representatives of TME. Noteworthy, the obtained EV-based formulations demonstrated the superior transfection efficacy compared to well-established transfection agent, GenePorter 3000. Overall, EVs offer distinct advantages that exceptionally position them as highly effective nucleic acids nanocarriers.

Results

Preparation and characterization of cationized EVs

The incorporation of a multivalent cationic lipid MVL5 (Fig. 1) was initially carried out at two different pH conditions, pH 7.4 and pH 6.3. For this purpose, various amounts of MVL5 were added to an aqueous dispersion of macrophage-derived EVs and the incorporation of the positively charged lipid into EVs was confirmed by zeta-potential measurements (Fig. 2A). Specifically, as the amount of MVL5 increased, the zeta-potential also increased from strongly negative values observed for naïve EVs to nearly neutral or slightly positive values for MVL5-EVs. At pH 7.4 incorporation of MVL5 was greater than at pH 6.3. For all further experiments, physiological conditions were selected.

The cationized EVs were purified from the excess of non-incorporated lipids by size exclusion chromatography or PEG precipitation. The zeta-potential distributions for the initial naïve EVs and modified EVs before and after purification (by PEG precipitation) were compared to confirm the incorporation of the MVL5 (Supplemental Fig. S1A–C). In all cases, EVs displayed uniform charge distribution. Of note, there was little if any difference in zeta-potential values before and after purification. The modified EVs were characterized by DLS and NTA (Fig. 2B and **C**). In the experiment when the amount of the cationic lipid was varied, at the relatively low excess of MVL5, the particles were characterized with effective diameters of ~150 nm and PDI ranging from 0.3 to 0.4. This was comparable to the characteristics of the unmodified EVs. However, at MVL5 amounts of 15 μg/10^{10} and higher, the particle size and PDI drastically increased suggesting the particle aggregation. Therefore, MVL5-EVs formulations prepared with low amount of the cationic lipid (0.01 μg/10^{10} particles – 15 μg/10^{10} particles) that allowed manufacturing relatively small nanoparticles with low PDI were chosen for further experiments. NTA measurements confirmed that incorporation of MVL5 under these conditions did not affect size and number of particles of cationized EVs at MVL5 2 μg/10^{10} particles (Fig. 2C) indicating that no aggregation occurred. Of

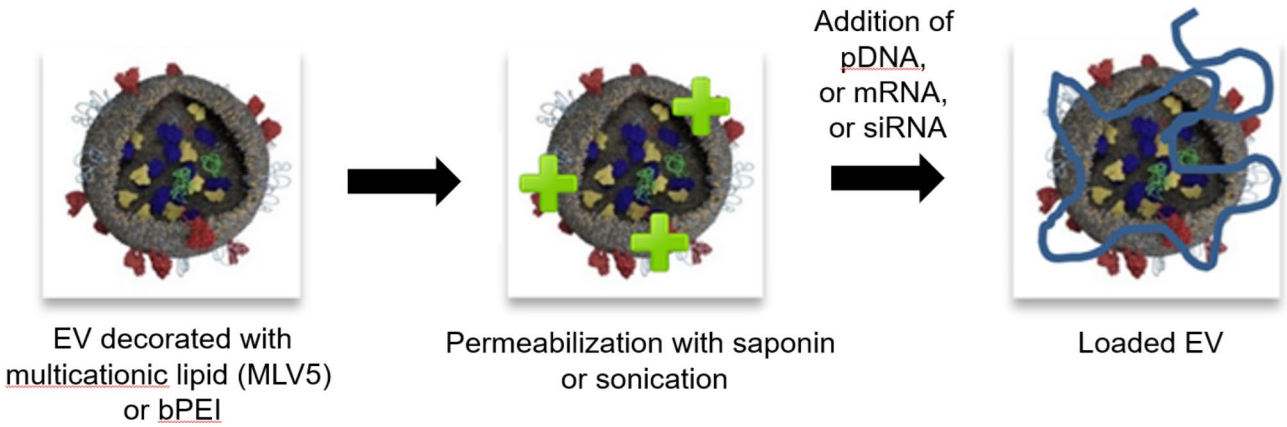

Fig. 1. Overall scheme for preparation of EV-nucleic acid nanoformulation.

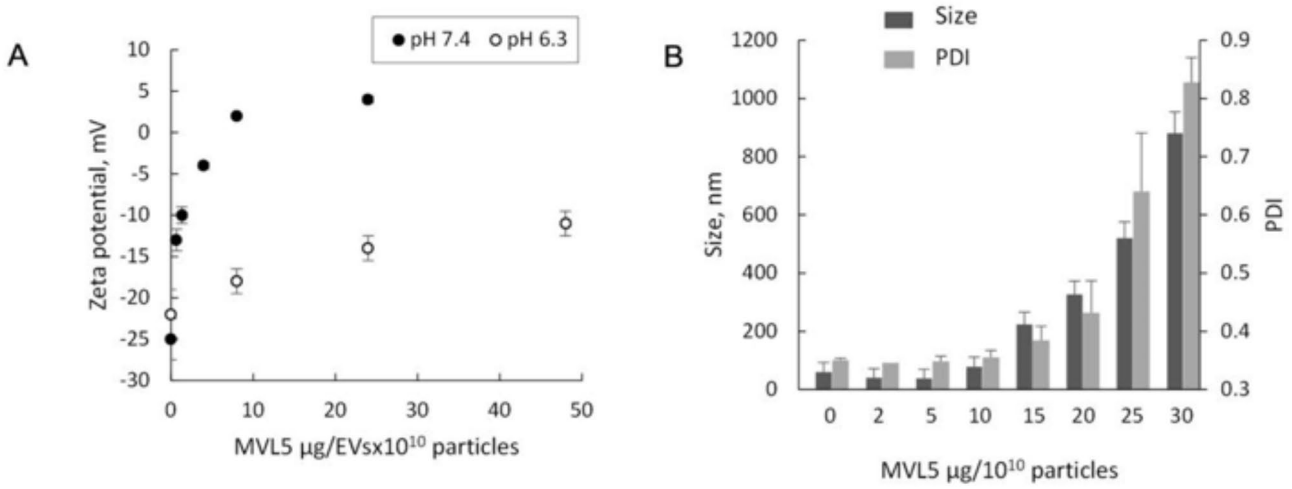

C

Formulation	Non-modified EVs	MVL5-EVs (sonication, PBS)	MVL5-EVs (sonication, EtOH)	MVL5-EVs (saponin, PBS)
Mean, nm	114.8 ± 8.3	128.0 ± 6.3	148.1 ± 12.0	125.0 ± 4.7
Mode, nm	110.5 ± 12.7	96.5 ± 7.4	110.0 ± 10.1	106.0 ± 8.2
Conc. x10^{10}	1.1	0.9	1.2	1.1

Fig. 2. Characterization of the MVL5 cationized EVs (MVL5-EV$_S$): (**A**) zeta-potential, (**B**) particle size and PDI by DLS and (**C**) particle size and concentration by NTA depending on the method of preparation of MLV5-EVs. The MLV5-EVs were prepared as indicated using EVs dispersed (**A**) in 10 mM phosphate buffer at pH 6.3 or (**A**, **B**) pH 7.4; and (**C**) in PBS or 50% PBS/EtOH solution with sonication or saponin permeabilization of EVs membranes. Addition of cationic lipid resulted in the increase of the (**A**) zeta-potential of EVs at both pH, and (**B**) size and PDI of the particles. The size and concentration of MLV5-EVs (2 µg/10^{10} particles) manufactured at various conditions were measured by NTA (**C**). Non-incorporated MLV5 was removed by size exclusion chromatography (**A**, **B**) or PEG precipitation (**C**) before the measurements.

note, addition of ethanol (EtOH) or saponin upon MVL5 incorporation did not significantly altered size and concentration of MVL5-EVs (Fig. 2C).

Manufacture of EV-Genes

The obtained cationized EVs carrying multivalent lipids in the membranes were then used to bind the negatively charged nucleic acids based on electrostatic interactions. The loading of nucleic acids (*p*DNA, mRNA, and siRNA) into cationized EVs was carried out by a simple co-incubation of nucleic acids with modified MVL5-EVs at room temperature (RT). The formation of the MVL5-EV-*p*DNA complex was confirmed by EtBr/*p*DNA fluorescence quenching. Intercalation of EtBr into *p*DNA is accompanied with a burst of the fluorescence. A quenching of EtBr fluorescence is commonly used to detect a formation of polyion complex between double stranded DNA and polycations. Various amounts of cationic lipid MVL5-EVs prepared by sonication at low amount of MVL5 (3.6 µg MVL5/10^{10} particles) were added to a mixture of EtBr (1 µg/mL) and *p*DNA (12.8 ng/µL), and fluorescence of EtBr/*p*DNA was recorded. The ratio of the fluorescence intensity in the presence (*I*) and absence of MVL5-EVs (*Io*) was plotted vs. concentration of MVL5-EVs (Fig. 3). The quenching of EtBr/*p*DNA fluorescence upon addition of cationized MVL5-EVs was observed. As the amount of MVL5-EV added to *p*DNA increased the *p*DNA/EtBr fluorescence quenched indicating the formation of the *p*DNA/MVL5 complex and the displacement of EtBr by the cationic groups of the lipid. Of note, a relatively small amount of MVL5 (3.6 µg/10^{10} EVs) was sufficient for binding nearly all *p*DNA added (12.8 ng/µL).

A similar procedure was used for loading siRNA to MVL5-EVs. In particular, fluorescently-labeled CY5-siRNA was added to cationized MVL5-EVs, and the obtained formulation (MVL5-EVs-CY5-siRNA) was purified from non-incorporated CY5-siRNA by size exclusion chromatography on Sepharose CL-4B (Supplemental Fig. S2A). The amount of siRNA in each fraction was determined by fluorescence (black circles), and the MVL5-EVs concentration - by NTA (red circles) (Supplemental Fig. S2A). Approximately 40% of all CY5-siRNA was eluted in a void volume along with MVL5-EVs. Of note, purification of MVL5-EVs/CY5-siRNA from non-incorporated CY5-siRNA by PEG precipitation produced similar results, specifically about 40% of CY5-siRNA was incorporated into cationized MVL5-EVs (Supplemental Fig. S2B).

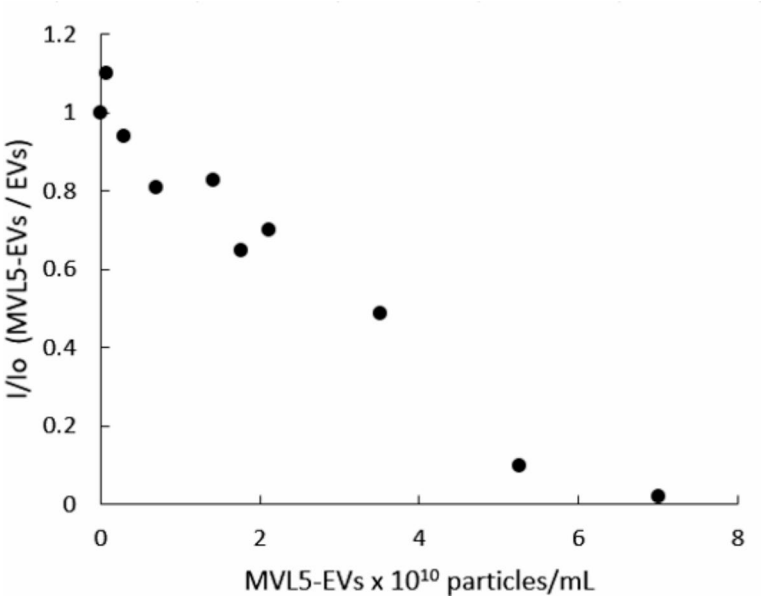

Fig. 3. Detection of *p*DNA compaction by EtBr displacement assay. The *p*DNA was mixed with EtBr and then titrated with MVL5-EVs. Sample fluorescence was determined after subtracting the baseline fluorescence of EtBr in the absence of *p*DNA. Data are presented as the ratio of fluorescence of EtBr (1 μg/mL) with *p*DNA (12.8 μg/μL) in the EVs with and without MVL5. Intercalation of EtBr into *p*DNA is accompanied with the increase of fluorescence quantum yield of the dye. Addition of the cationic lipid MVL5 results in the quenching of the fluorescence due to the displacement of EtBr by the MVL5.

Delivery of functional nucleic acids to target cells by cationized EVs

Efficient delivery of therapeutic genes to target cells is crucial for the therapeutic application of *p*DNA. Therefore, we studied accumulation and trafficking of fluorescently labeled YOYO-1 *p*DNA formulated with cationized EVs in RAW 264.7 macrophages. Polyethyleneimine (PEI) was employed for initial experiment for trafficking of fluorescently labeled YOYO-1 *p*DNA. PEI is a commonly used cationic polymer for nucleic acid delivery due to its high density of positive charges, also worth point that it is much cheaper than cationic lipid. For PEI-EVs production, the same exosomes as for the rest of the experiment were used. The macrophages were incubated with complexes of the *p*DNA and cationized PEI-EVs for different time points, and the intracellular distribution of the plasmid was studied by confocal microscopy (Fig. 4). The obtained images suggested that *p*DNA accumulated in the cells, over time. Noteworthy, a considerable amount (ca. 59.2 ± 3.4%) of *p*DNA (green) was co-localized with nuclei (here red) at 240 min as was manifested in yellow staining.

Next, the accumulation of MVL5-EVs/CY5-siRNA formulations in triple negative breast cancer (TNBC) cells MDA-MB-231 was studied by confocal microscopy (Fig. 5). Little if any fluorescence of CY5-siRNA was detected in cancer cells incubated with the naked siRNA (Fig. 5A), or a mixture of siRNA and naïve non-

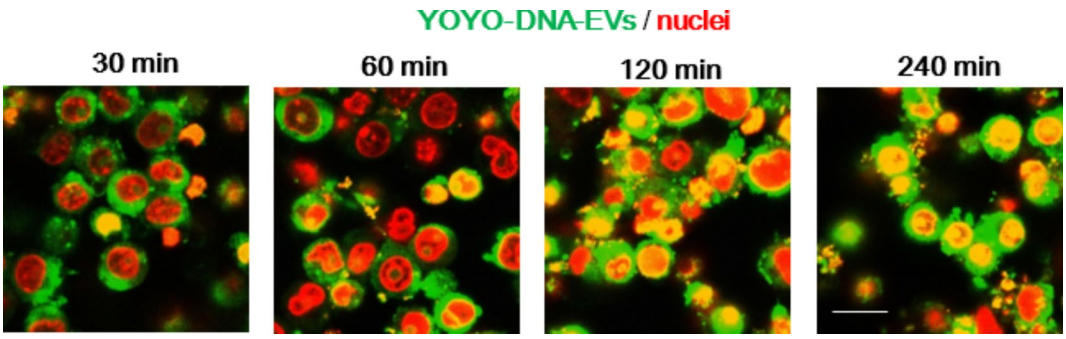

Fig. 4. Intracellular distribution of cationized EVs-*p*DNA. YOYO-labeled *p*DNA (here green) was loaded into EVs and purified by PEG precipitation. Cationized EVs-YOYO-*p*DNA (1×10^{11} particles/mL) was added to RAW 264.7 macrophages for various time points. Following incubation, the cells were washed with PBS, and nuclei were stained with Hoechst (here red). Significant co-localization of *p*DNA and nuclei staining was recorded over 240 min, indicating that EVs delivered *p*DNA to the nuclei. *p*DNA (1.6 μg/μL); EVs (1×10^{11} particles); cationic lipid, PEI (27 mg/mL) PEI was incorporated into EVs by transient permeabilization with saponin as described in Materials and Methods. The bar: 20 μm.

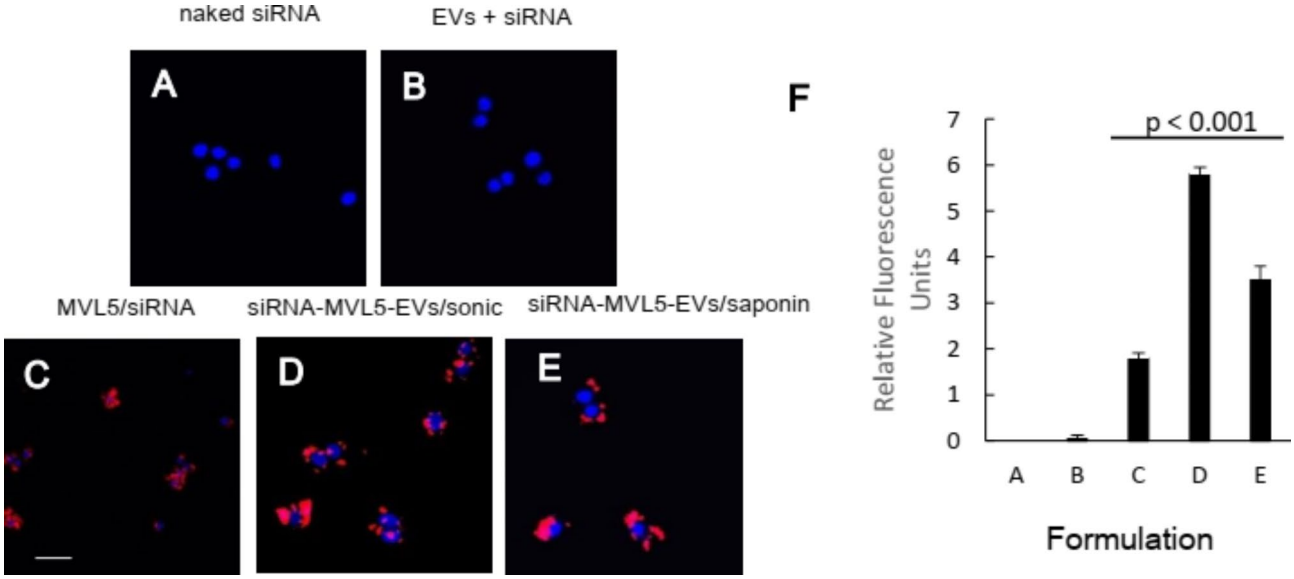

Fig. 5. Accumulation of MVL5-EVs/CY5-siRNA in cancer cells. MDA-MB-231 cells (1×10^4 cells/well) were incubated with: **(A)** CY5-siRNA alone (1 nmol/well, red), **(B)** mixture of CY5-siRNA and non-modified EVs, **(C)** MVL5 lipid and siRNA, **(D)** siRNA loaded into MVL5-EVs (10 µg MVL5/10^{10} particles) by sonication, and **(E)** siRNA loaded into MVL5-EVs (the same number of particles) by saponin. The nuclei were stained with Hoechst (blue). **(F)** The mean fluorescence intensity of CY5-siRNA in the cells was determined. After MVL5 incorporation into EVs by sonication or saponin permeabilization, MVL5-EVs were purified by column chromatography, mixed with CY5-siRNA, and then purified again. The bar: 20 µm.

modified EVs (Fig. 5B). In contrast, formulations of CY5-siRNA with cationized MVL5-EVs obtained by sonication (Fig. 5D) or saponin permeabilization (Fig. 5E) displayed significant accumulation in cancer cells, and specifically in nuclei (~ 47%). As expected, the formation of MVL5/siRNA complex in the absence of EVs also promoted siRNA accumulation in cancer cells (Fig. 5C), although to a lesser extent than in the presence of EVs nanocarriers. The levels of accumulated siRNA were accounted by fluorescence intensity (Fig. 5F).

Transfection of cancer cells by *p*DNA loaded into cationized MVL5-EVs

MVL5-EV-based formulations of Luc-encoding *p*DNA with optimal size and loading efficiency described above were utilized for transfection of IC21 macrophages in vitro. For this purpose, MVL5-EVs with various amounts of cationic lipid, which was incorporated with or without EtOH were loaded with the Luc-*p*DNA, and the expression of the encoded protein was assessed by luminescence (Fig. 6). First, a crucial role of temperature upon the first step of preparation (MVL5 incorporation) on transfection efficacy was observed (Fig. 6A). The highest transfection efficiency was recorded with formulation obtained at 42 °C. We hypothesized that there may be a number of reasons for this effect. First, when temperature increased from 35 °C to 42 °C, a fluidization of membrane might result in facilitation of hydrophobic lipid chains incorporation into the EVs membranes. Further increase of temperature (from 42 °C to 52 °C) might lead to the disruption of lipid rafts and other ordered domains within the lipid bilayer, resulting in a transition to a fully fluid state. This change can cause denaturation of surface proteins, alterations in EVs surface topography, and particle aggregation. In fact, we recorded drastic increase in the particles diameter upon temperature increases, specifically from 120 nm at 42 °C to 600 nm at 52 °C. This resulted in the less accumulation of *p*DNA-loaded MVL5-EVs in the IC21 macrophages and decreases in transfection efficacy at 52 °C (Fig. 6A).

Next, as the amount of MVL5 incorporated into EVs increased the transfection efficacy also increased, while the luminescence signals in cells incubated with the naked *p*DNA or *p*DNA and naïve EVs mixture did not exceed background levels (Fig. 6B). The Luc expression levels were significantly greater in the cells transfected with MVL5-EVs-*p*DNA compared to the cells transfected with the same amount of MVL5/*p*DNA polyion complex (at the same lipid and *p*DNA concentrations). The treatment of cells with most efficient MVL5-EVs- Luc-*p*DNA formulation (40 µg MVL5/10^{11} EVs obtained in the presence of EtOH) resulted in even greater transfection performance than that observed using commercially available GenePorter 3 K (GP3K). Noteworthy, addition of EtOH upon cationic lipid incorporation into EVs significantly increased transfection efficiency compared to modification of EVs with the same amount of MVL5 in PBS (Fig. 6B).

The expression of the green fluorescent protein (GFP), and intracellular accumulation of *p*DNA and cationized EVs were recorded using *p*DNA encoding GFP in Raw 264.7 macrophages (Fig. 7).

GFP-*p*DNA (orange) loaded into cationized EVs (red) was efficiently transported to RAW 264.7 cells resulting in the expression of the GFP (green). The accumulation of cationized EVs-*p*DNA formulation, and GFP expression levels increased over time.

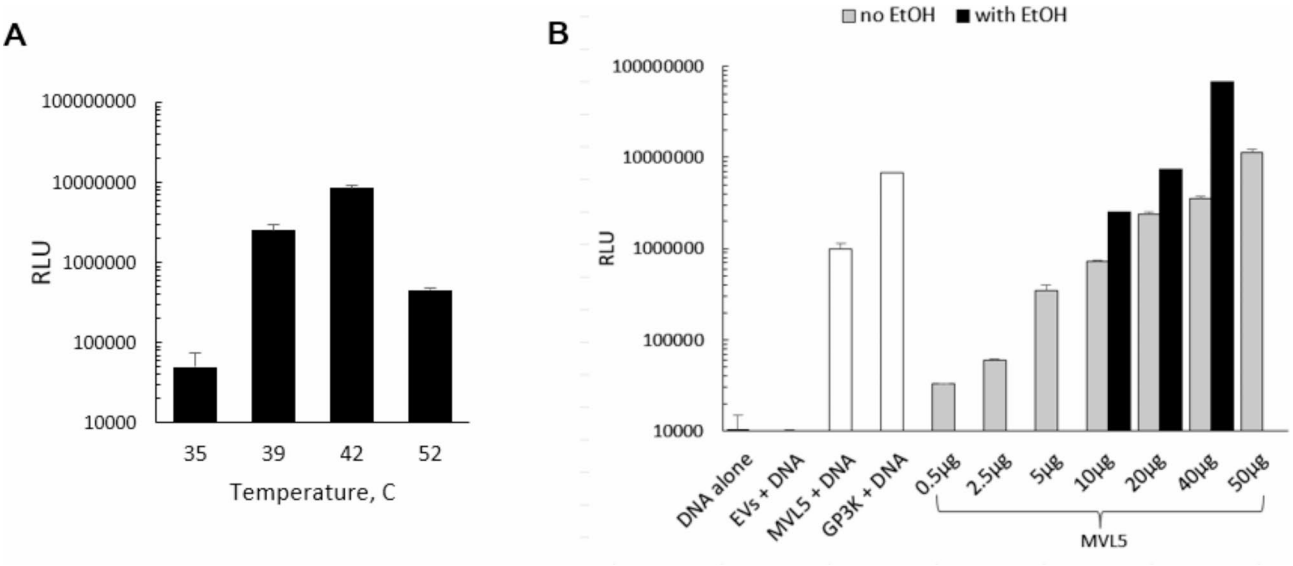

Fig. 6. Transfection of IC21 macrophages with MVL5-EVs-based formulations of *p*DNA. (**A**) MVL5-EVs (20 μg MVL5/10^{11}particles) were prepared *via* MVL5 incorporation into EVs by sonication at different temperatures (PEG purification after MVL5 incorporation), and then loaded with luciferase *p*DNA (6 μg /10^{11}particles). IC21 macrophages (1×10^5 cells/well) were supplemented with MVL5-EVs formulations of *p*DNA (1×10^{10} particles/1 μg *p*DNA/well) and incubated for 4 h at 37 °C. (**B**) MVL5-EVs were prepared *via* incorporation of different amounts of MVL5 (0.5–50 μg MVL5/10^{11}particles) into EVs by sonication in the presence or absence of EtOH (50%) and added to IC21 macrophages (2×10^4 cells/well). Free *p*DNA (1 μg/well), or mixture of EVs and *p*DNA (10^{10}particles/1 μg *p*DNA/well), or mixture of common transfection agent, GenePorter (GP3K, according to manufacturer's protocol), with *p*DNA (1 μg/well) at the same concentration were used as controls. Then, the cells were washed with PBS and cultured in full media for 24 h, and the luminescence of lysed cells in the presence of luciferin-ATP was measured. White bars – samples without EVs. (**A**) Bell shaped curve was observed for transfection efficacy with maximum at 42 °C used for cationized EVs preparation. (**B**) Transfection efficacy increased with the increases of MVL5 incorporated into EVs nanocarriers. Little, if any, luminescence was detected in cells exposed to naked *p*DNA, or mixture *p*DNA with non-cationized EVs. As expected, significant transfection was observed in the cells supplemented mixture of free *p*DNA and the cationic lipid, or free *p*DNA and GP3K.

Transfection of cancer cells by mRNA loaded into cationized MVL5-EVs

Optimal transfection conditions determined for MVL5-EVs-*p*DNA formulations were then utilized for transfection of IC21 macrophages with Luc-encoding mRNA loaded into MVL5-EVs (Fig. 8). Similar to EVs-based formulations of *p*DNA, increases in the amount of mRNA incorporated into MVL5-EVs resulted in the increased transfection efficacy, however, the levels of luminescence in the cells transfected with MVL5-EVs-Luc-mRNA formulation were lower than those transfected with MVL5-EVs-Luc-*p*DNA (Fig. 6B). This could be due to several reasons, such as the difference in the optimal concentrations of mRNA and *p*DNA, or faster mRNA degradation in the cells compared to *p*DNA degradation.

Knockdown of luc by MVL5-EVs-siRNA in cancer cells

Successful knockdown of Luc by siRNA loaded into MVL5-EVs was achieved in Luc-overexpressing TNBC cells, Luc-MDA-MB-231. Significant decreases of luminescence were detected in cells treated with MVL5-EVs-siRNA formulation for 24 h (Fig. 9A). Of note, siRNA alone, or mixture of naive EVs and siRNA, or MVL5-EVs without siRNA did not have any significant effect on Luc expression. Furthermore, as the amount of siRNA in the formulation increased the efficiency of Luc knockdown by MVL5-EVs-siRNA also increased (Fig. 9B).

Discussion

Efficient delivery of nucleic acids to the site of disease is the main hurdle for using these powerful therapeutics. Multiple natural mechanisms were developed to protect cells from altering their functions that successfully work in healthy body. However, in case of disease, it is crucial to deliver therapeutic genes and restore correct functions. Different approaches were developed to protect and deliver genes to the affected tissues. One of the promising tools is formulation of nucleic acids into synthetic nanoparticles, which provide gene protection, prolonged circulation, and in some cases targeting to a disease side. However, the opsonization of drug-loaded nanoparticles in the bloodstream causes rapid drug clearance by the mononuclear phagocyte system (MPS). In contrast, EVs are biocompatible and biodegradable natural nanocarriers, and have low immunogenicity and toxicity that, along with their membranotropic nature, can improve delivery of incorporated drugs to target cells, ultimately increasing drug therapeutic efficacy.

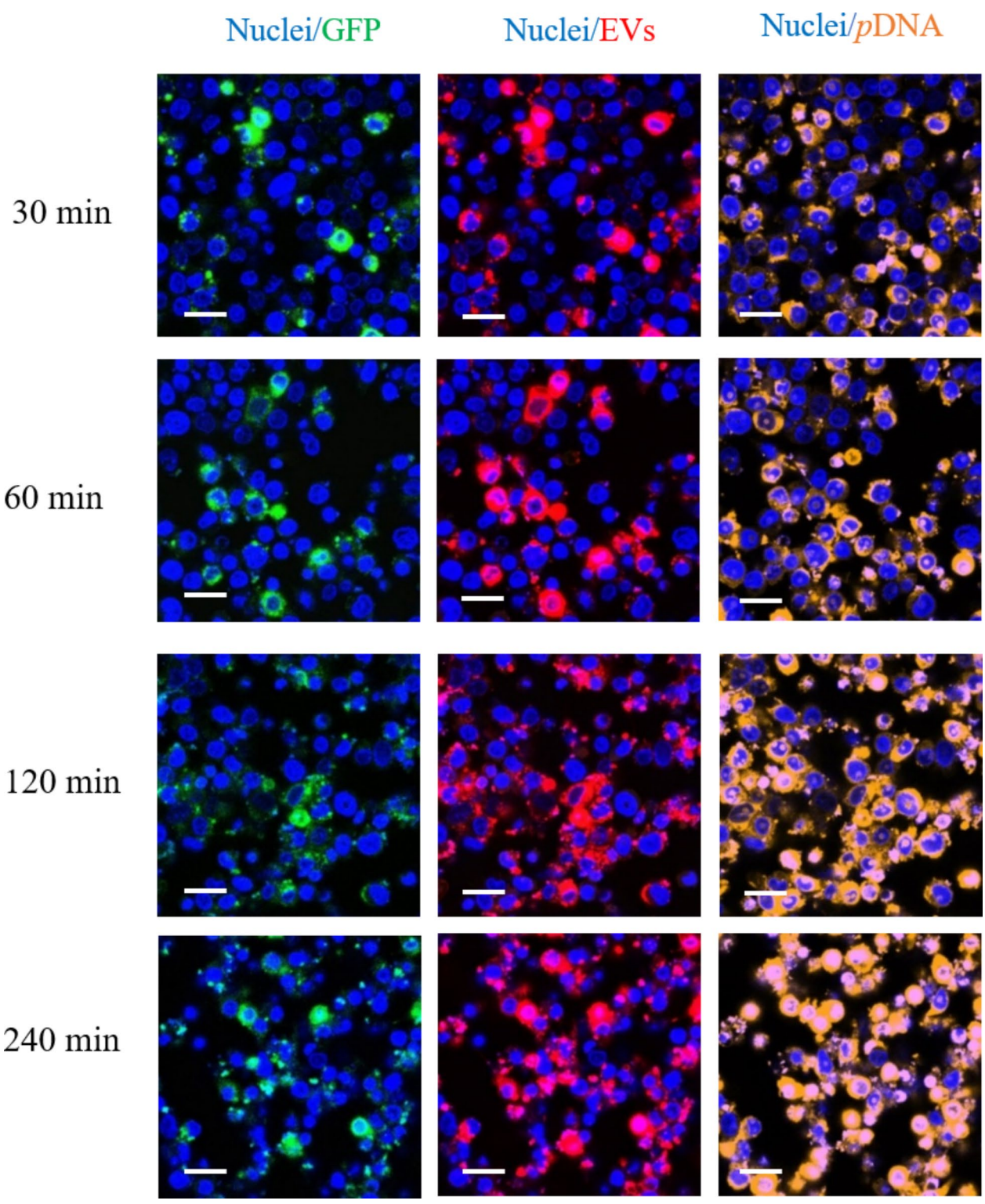

Fig. 7. Accumulation of cationized EVs loaded with GFP-pDNA, and the expression of the encoded protein in Raw 264.7 macrophages. Cationized EVs were labeled with fluorescent dye, DID (red) and GFP-encoding *p*DNA was labeled with nucleic acid fluorescent dye, TOTO (orange, ex/em 514/533). Raw 264.7 macrophages (5×10^4 cells/well) were supplemented with cationized EVs loaded with GFP-*p*DNA (10^{10} particles/1μg *p*DNA/well) for various times, and intracellular distribution of all components of the formulation, as well as the expression of the encoded protein, GFP, was examined by confocal microscopy. The nuclei were stained with Hoechst (blue). Considerable amount of cationized EVs, as well as TOTO-*p*DNA was detected in Raw 264.7 macrophages over 240 min. The expression of GFP was increased at later time points (120–240 min). Cationized EVs were obtained by EVs supplemented with PEI by saponin permeabilization, followed by PEG purification. The bar: 20 μm.

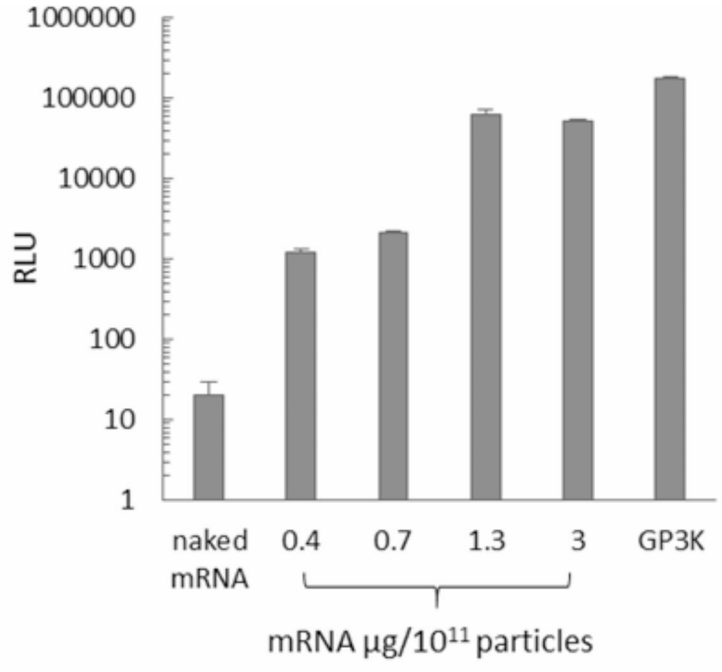

Fig. 8. Transfection IC21 macrophages with MVL5-EVs-luc-mRNA. MVL5-EVs (20 µg MVL5/10^{11}particles) were prepared *via* MVL5 incorporation into EVs by sonication at 42 °C with PEG purification after MVL5 incorporation, and then loaded with luciferase mRNA (1.3 µg /10^{11} particles). IC21 macrophages (1×10^5 cells/well) were supplemented with MVL5-EVs-Luc-mRNA (3 µg/10^{11} particles/well) loaded with different amount of mRNA (0.4–3 µg) and incubated for 4 h at 37 °C. Naked mRNA (maximum amount, 3 µg/well) with or without GP3K was used as a control. Then, the cells were washed with PBS and cultured in full media for 24 h, and the luminescence of lysed cells in the presence of luciferin-ATP was measured. Cationized EVs provided efficient transfection in vitro. MVL5-EVs were obtained by lipid incorporation using sonication in water bath followed by PEG precipitation.

Herein, we report the development of EV-based drug delivery system for nucleic acids (EV-Genes). To attain strong interactions between negatively charged nucleic acids and EVs, these nanocarriers were modified with positively charged multivalent lipid, MVL5. Efficient incorporation of MVL5 into EVs was confirmed by zeta potential measurements before and after purification using column chromatography or PEG precipitation. The modification of cationized EVs considerably decreased their negative charge and increased their size. The co-incubation of nucleic acids with these MVL5-EVs resulted in successful loading of *p*DNA, or mRNA, or siRNA.

Next, efficient delivery of nucleic acids to the target cells in vitro was confirmed by confocal microscopy. In particular, fluorescently labeled *p*DNA was accumulated in RAW 264.7 macrophages, and co-localized (~ 60%) with nuclei. Furthermore, significant accumulation of fluorescently labeled siRNA loaded into cationised EVs was detected in triple negative breast cancer cells, while siRNA alone or mixture of siRNA and non-cationized EVs were not detected.

Noteworthy, loading of *p*DNA and mRNA to cationized MVL5-EVs resulted in efficient transfection of target cells. First, we demonstrated that the greater amount of cationic lipid MVL5 was incorporated into EVs, the greater transfection efficacy was achieved. We speculate that several different factors might play a role in this process: *i*) stronger interactions of nucleic acids with the cationized MVL5-EVs; or/and *ii*) greater proton sponge effect that allows endosomal escape of incorporated nucleic acids. Furthermore, using EtOH at the first step of lipid incorporation resulted in higher transfection levels. This might be also due to the better incorporation of MVL5 into EVs membrane. Finally, the optimization of temperature during lipid incorporation into EVs resulted in greater transfection levels. We hypothesized that increase in temperature from 35 °C to 42 °C caused fluidization of EVs membrane followed by more efficient incorporation of hydrophobic part of MVL5 molecule. However, further increase in temperature up to 52 °C might lead to protein denaturation in EVs membranes, their aggregation, and as a result, decrease for MVL5 incorporated. Of note, transfection of the cells with *p*DNA-MVL5-EVs was greater than with mRNA-MVL5-EVs. We hypothesized that this might be due to the higher stability of *p*DNA compared to mRNA. Finally, efficient knockdown of Luc in target triple negative breast cancer cells was demonstrated with optimal siRNA-MVL5-EVs formulations. Overall, the manufacture of multivalent cationized EVs allowed efficient loading of different nucleic acids (*p*DNA, mRNA, and siRNA) and delivery to target cells. As result, successful transfection with these MVL5-modified EV-*p*DNA and EV-mRNA and knockdown with EV-siRNA was achieved. This may be a powerful approach for delivery of therapeutic genes in clinic.

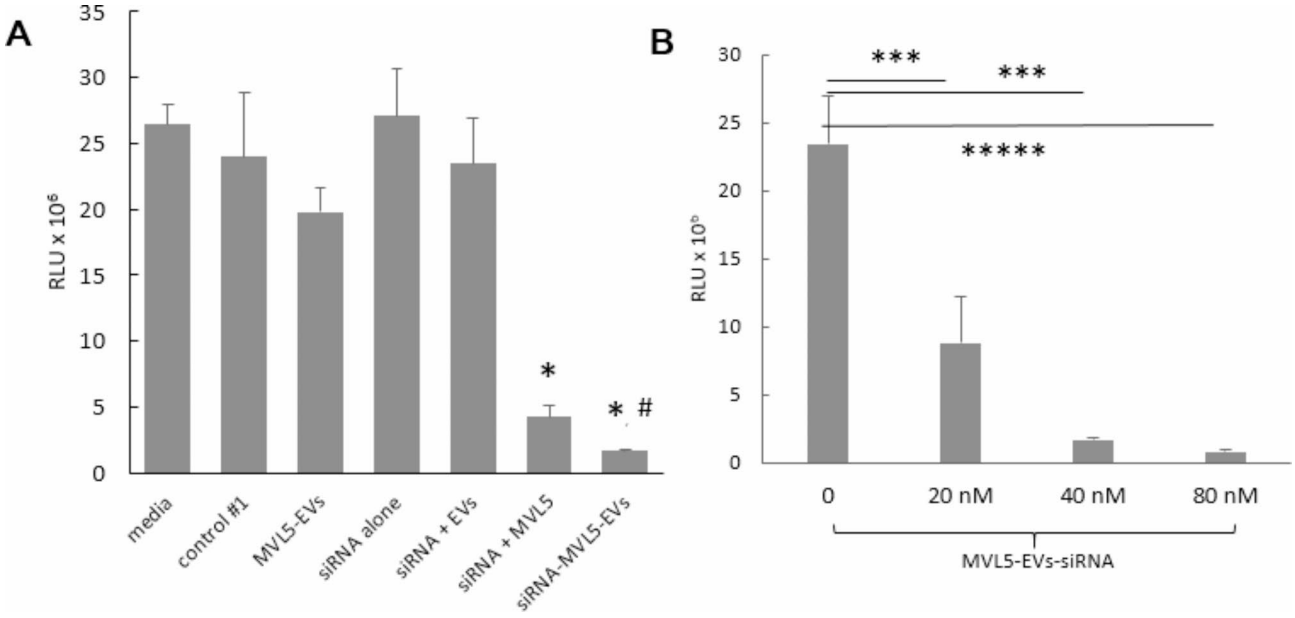

Fig. 9. Knockdown of Luc by MVL5-EVs-siRNA in Luc-MDA-MB-231 cancer cells. (**A**) MVL5-EVs (12 μg MVL5/10^{10}particles) were prepared *via* MVL5 incorporation into EVs by sonication at 42^0C with PEG purification after MVL5 incorporation, and then 65 μL of MVL5-EVs were loaded with GL2 + GL3 siRNA (0.6 μM /10^{10} particles). Previously transfected MDA-MB-231 cells (Luc-MDA-MB-231) (1×10^4 cells/well) were supplemented with MVL5-EVs loaded with GL2 + GL3 siRNA (1.3 μg MVL5/10^9 particles/40 nM siRNA/well) and incubated for 4 h at 37 °C. Then, cells were washed and cultured in complete media for 24 h. Free siRNA, or mixture siRNA with EVs, or MVL5-EVs without siRNA, or mixture of siRNA and MVL5, or scrambled siRNA (control #1) at same concentrations were used as controls. Free media was also used as control. The luminescence was measured in cell lysates. Significant knockdown of Luc was recorded in the cells incubated by MVL5-EVs-siRNA. *$p < 0.0001$ compared to media; #$p < 0.001$ compared to siRNA mixed with MVL5. (**B**) MVL5-EVs (12 μg MVL5/10^{10}particles) were prepared *via* MVL5 incorporation into EVs by sonication at 42^0C with PEG purification after MVL5 incorporation, and then 65 μL of MVL5-EVs were loaded with GL2 + GL3 siRNA at different concentrations of siRNA (0.6 μM, 1.23 μM, or 2.46 μM). Luc-MDA-MB-231 cells (1×10^4 cells/well) were supplemented with different concentrations of MVL5-EVs loaded with GL2 + GL3 siRNA (up to 80 nM siRNA) and incubated for 4 h at 37^0C. Then, cells were washed and cultured in complete media for 24 h. Increases in siRNA amount in MVL5-EVs formulation resulted in the greater knockdown of the target protein ***$p < 0.00005$; ****$p < 0.000005$ compared to Luc-MDA-MB-231 with scramble siRNA, the first bar on the graph.

Materials and methods

Reagents and materials

Recombinant *p*DNA and mRNA encoding Luciferase (Luc) and *p*DNA encoding green fluorescent protein (GFP) were obtained from Genlantis Inc. San Diego, CA, USA. Cyclin-dependent kinase regulatory subunit (CLB1) siRNA-Cy5 (PARLL-000041, Dharmacon) was purchased from Healthca, GE, USA. Silencer firefly Luc (GL2 + GL3) siRNA (cat #AM4629) was purchased from Ambion, Inc., Foster City, CA, USA. Multivalent cationic lipid N1-[2-((1 S)-1-[(3-aminopropyl)amino]-4-[di(3-amino-propyl)amino]butylcarboxamido) ethyl]-3,4-di[oleyloxy]-benzamide (MVL5) was from Avanti Polar Lipids, Inc. (Alabaster, AL, USA). Cationic copolymer, branched polyethyleneimine (PEI) with 48 primary amino groups was purchased from Sigma-Aldrich (St. Louis, MO, USA). A lipophilic fluorescent dyes, 2-(5-(1,3-dihydro-3,3-dimethyl-1-octadecyl-2 H-indol-2-ylidene)-1,3-pentadienyl)-3,3-dimethyl-1-octadecyl-perchlorate (DID), 1,1'-dioctadecyl-3,3,3',3'-tetramethylindocarbocyanine perchlorate (DIL), TOTO-1 Iodide and YOYO-1 Iodide were purchased from Invitrogen (Carlsbad, CA, USA). Polyethylene glycol (8 kDa, PEG), saponin, Triton X-100, Sepharose CL-4B, phosphate-buffered saline (PBS), and EtOH were obtained from Sigma-Aldrich (St. Louis, MO, USA). GenePORTER 3000 transfection agent was purchased from AMS Biotechnology (Milton, Abingdon, UK). Cell lysis buffer (Promega) was used for preparation of cell lysate in the experiments.

Cells

Mouse macrophage cell lines (Raw 264.7, and IC21), and TNBC cells MDA-MB 231, were purchased from ATCC (Manassas, VA, USA). Luc-MDA-MB-231 cell line was a generous gift from Dr. Leslie Parise, Chair of the Department of Biochemistry and Biophysics at UNC. Cells were cultured in Dulbecco's Modified Eagle's Media (DMEM) (Invitrogen) supplemented with 10% (v/v) heat-inactivated fetal bovine serum (FBS), and 1% (v/v) of both penicillin and streptomycin. The cells were grown in an incubator with optimal culture conditions of 37 °C and 5% CO_2, and the medium was routinely replaced every 2–3 days.

Isolation of EVs

For all studies, EV-depleted media was prepared by ultracentrifugation of fetal bovine serum (FBS) at 120,000 x g for 110 min to remove all vesicular content prior to addition to media.

Concomitant media from parental cells, IC21 macrophages, grown on 75T flasks (20×10^6 cells/flask) was collected, and EVs were isolated using PEG precipitation. In brief, the culture supernatants were cleared of cell debris and large vesicles by sequential centrifugation at 1000 x g for 10 min, and 10,000 x g for 15 min, followed by filtration using 0.2 μm syringe filters. Then, the cleared sample (20 mL) was supplemented with 40% PEG (8 mL) and incubated at 4 °C overnight. After that, the samples were spun at 4,700 x g for 30 min to pellet the EVs, and supernatant was discarded. The pellet was re-suspended with 250 μL PBS.

Characterization of EVs

The collected EVs (10^{11} – 10^{12} EVs/flask) were washed twice with PBS and stored at – 80° C. The EVs were characterized by measuring: (1) the protein concentration using the Bradford assay, (2) the size and particles concentration using Nanoparticle Tracking Analysis (NTA), and (3) the size and polydispersity index (PdI) using Dynamic Light Scattering (DLS).

NTA. EVs were characterized by NTA using NanoSight NS 500 (Malvern, UK). The settings were optimized and kept constant between samples, and each video was analyzed using the Nanosight NTA 3.2 software to obtain the size and concentration of EVs. The stability of EVs was monitored by measuring size over a period of time at 4 °C, room temperature (RT), or 37 °C. Prior to the measurements EVs were diluted to yield particles concentration to approximately 10^8 particles/mL. All samples were analyzed five times.

Dynamic Light Scattering (DLS). The average hydrodynamic diameter and zeta potential of EVs was measured by DLS using a Malvern Zetasizer Nano ZS system (Malvern, Worcestershire, UK) equipped with He–Ne laser (5 mW, 633 nm) as the light source at 22 °C. All samples were analyzed in triplicate.

Preparation of cationized EVs

EVs secreted by macrophages were modified with cationic multivalent lipid, MVL5, or cationic branched polymer, polyethyleneimine (PEI) by two methods: (1) using aqueous media (PBS or phosphate buffer), or (2) 50% PBS/EtOH solution. For MVL5 incorporation using the first procedure, various amounts (1–16 μl) of MVL5 in EtOH (5 mg/mL) was added to the isolated EVs (10^9-10^{12} particles/mL) dispersed in PBS, pH 7.4; or 10 mM phosphate buffer, pH7.4; or pH 6.3. In selected cases immediately before the addition of the lipid, EVs were treated with saponin (2 mg/ml) to permeabilize the membranes. In the second procedure, the same amount of MVL5 in EtOH was added to EVs in 50% wt. PBS/EtOH solution. The resulting mixtures were incubated at different conditions (RT, or sonicated bath for 10 min at 35 °C, 42ºC, or 52 °C), and then incubated at RT for one hour to allow the membrane relaxation. The same method was used for incorporation of PEI into EVs. In both cases, cationized EVs were purified from non-incorporated cation by size-exclusion chromatography on Sepharose CL-4B (Sigma), or using PEG precipitation as described above.

Preparation of nucleic acid and MVL5-EVs nanoformulations

As a general procedure 2.5 μl Luc-encoding *p*DNA (1.6 μg/μL) in water or 4 μL Luc-mRNA (1 μg/μL) in water were added to 400 μl MVL5-EVs (5×10^9 – 5×10^{11} particles/mL) in serum-free media, and incubated for 15 min upon gentle mixing at RT. In particular, for loading of siRNA, 500μL of MVL5-EVs (10 μg MVL5/10^{10} particles/mL) obtained by sonication, or saponin permeabilization (at room temperature (RT)) were supplemented dropwise with CLB1 CY5-siRNA (20 μM, 30 μL) in siRNA buffer (60 mM KCl, 6 mM HEPES, pH 7.5, 0.12 mM $MgCl_2$) and vortexed for 30 s. The mixture was incubated for 1 h at 37 °C, and MVL5-EVs with incorporated siRNA were purified from non-incorporated siRNA on a Sepharose CL-4B column (3.7 mL diameter 1 cm). Purified EVs were collected in 8 fractions (0.5 mL each), and the level of fluorescence (CY5) in EVs fractions was measured on 96-well-black clear bottom plate ($\lambda_{ex}=649$, $\lambda_{em}=675$).

Ethidium bromide (EtBr) titration assay

For the EtBr titration assay, MVL5 (2.5 μg /100 μL) was added to EVs (7×10^9 particles/100 μL), then subjected to sonication and purified by PEG precipitation as described above. Serial dilutions of MVL5-EVs in PBS (100 μL total volume) were supplemented with a mixture of 4 μL EtBr (25 μg/mL), and 0.8 μL *p*-DNA (1.66 μg/μL). The obtained mixture was incubated at RT for 10 min, and fluorescence of EtBr ($\lambda_{ex}=525$, $\lambda_{em}=605$) was measured in the presence and absence of *p*DNA. The data were expressed as a ratio between fluorescence intensity of EtBr/DNA in the presence (I) and absence (I_0) of MVL5-EVs.

Accumulation of EVs formulations of nucleic acids in cancer cells

To study siRNA accumulation, MDA-MB-231 cells (1×10^4 cells/well) were plated in 8-chamber slide one day prior to experiment. MVL5-EVs/CY5-siRNA and all relevant controls (EVs/CY5-siRNA siRNA; CY5-siRNA siRNA/MVL5; and CY5-siRNA siRNA alone) were prepared immediately prior to experiment in sterile PBS. The cells were incubated with siRNA formulations (1 nmol siRNA/well) for 4 h in serum-free media (SFM), washed thrice with PBS supplemented with 1 mg/mL heparin sulfate to remove unbound complexes; and fixed for 15 min at RT in 4.0% paraformaldehyde (PFA). Then, the cells were stained with 1:5000 dilution of Hoechst nucleic acid counterstain, rinsed 3X, supplemented with 200 μL of PBS, and imaged on Zeiss 710 Confocal Microscope with argon ion laser and corresponding filter set. Digital images were obtained using the CCD camera (Photometrics) and Adobe Photoshop software. The mean intensity of siRNA in the cells was analyzed by ImageJ software. To calculate the mean fluorescence intensity for each treatment group, the fluorescent images from multiple fields of view were assessed for fluorescent areas, and the average of these values was calculated. The comparison was performed on 7–10 sets of images acquired with the same optical settings.

Intracellular distribution of YOYO-labeled cationized EVs in raw 264.7 macrophages

*p*DNA was labeled with a fluorescent dye, YOYO according to manufacturer's protocol, and YOYO-labeled *p*DNA (1.6 μg/μL) was loaded into cationized with PEI EVs (1×10^{11} particles) and purified by PEG (40%) precipitation. Cationic lipid, PEI (27 mg/mL) was incorporated into EVs by transient permeabilization with saponin (2 mg/ml, 0.27% final concentration for 15 min). Cationized EVs-YOYO-*p*DNA (1×10^{11} particles/mL) was added to RAW 264.7 macrophages seeded on slides (2×10^6 cells/chamber) for various time points (30–240 min). Following the incubation, the cells were washed with PBS, and nuclei were stained with Hoechst. Hoechst nucleic acid counterstain, rinsed 3X, supplemented with 200 μL of PBS, and imaged on Zeiss 710 Confocal Microscope with argon ion laser and corresponding filter set. Digital images were obtained using the CCD camera (Photometrics).

Transfection of cells with EVs-*p*DNA or EVs-mRNA

Transfection efficacy of EVs-*p*DNA and EVs-mRNA in vitro was evaluated in Raw 264.7 and IC21 macrophages. MVL5-EVs isolated by PEG precipitation were rehydrated in serum-free media (SFM) and Luc-encoding *p*DNA (1.6 μg/μL) or mRNA (1 μg/μL) were loaded by gentle mixing at RT as described above. Macrophages were seeded onto 24-well plate (1×10^5cells/well) overnight, then the media was substituted for SFM, and MVL5-EVs-*p*DNA or MVL5-EVs-mRNA were added to the cells (1 μg/well for *p*DNA and 3.3 μg/well for mRNA). In one control experiment, the cells were incubated with a mixture of Luc-encoding *p*DNA (1.6 μg/μL) and GenePORTER 3000 in SFM according to manufacturer's protocol. The cells were incubated for 4 h with either cationized EVs-*p*DNA or EVs-mRNA, then media was removed, and cells were cultured in complete media (10% FBS and 1% penicillin/streptomycin) for 24 h. Then, cells were lysed and the levels of luminescence were measured with luciferin/Luc mixture on Glomax 20/20 Luminometer (Promega). The luminescence levels were normalized by the protein content.

To study accumulation and transfection of cancer cells by confocal microscopy, 10 μL GFP-encoding *p*DNA (800 ng/μL) was supplemented with 1 μL TOTO-1 Iodide and incubated for 15 min. After that 11 μL fluorescently labeled *p*DNA was added to cationized EVs (10 μg PEI/10^{11} particles/mL, obtained by sonication in water bath at 42 °C, followed by PEG purification) for 15 min and the resulted formulation was supplemented with a second label DIL for another 15 min. Raw 264.7 macrophages (1×10^5 cells/well) were seeded overnight into chambers and 100 μL of EVs-*p*DNA was added to each chamber and 400 μL serum-free DMEM media. Cells were incubated at 37 °C for 30 min, 60 min, 120 min, and 240 min, and then the media was replaced with 500 μL fresh full media. The cells were washed, fixed, and permeabilized with formaldehyde. The nuclei were stained with Hoechst for 2 min and rinsed with PBS. The expression of GFP was examined by confocal microscopy on Zeiss 710 Confocal Microscope with argon ion laser and corresponding filter set.

Knockdown of Luc expression with MVL5-EVs-siRNA

To prepare MVL5-EVs, 200 μl of MVL5 solution in EtOH (0.2 mg/mL or 0.4 mg/mL) was added to 200 μL IC21 macrophage-derived EVs suspension (3.2×10^{11} particles/mL), and sonicated in water bath for 15 min at 45 °C. Then, obtained EVs suspension was incubated at RT for 1 h for membrane relaxation, and purified from non-incorporated lipid by PEG precipitation. The pellet was rehydrated in 200 μL in serum-free media, and then 65 μL of MVL5-EVs were supplemented with GL2 + GL3 siRNA (0.6 μM, 1.23 μM, or 2.46 μM) and incubated for 15 min at RT. The obtained MVL5-EV/GL2 + GL3 siRNA formulation was used in knockdown experiments.

Luc-MDA-MB-231 cells (1×10^4 cells/well) were seeded into 96-well plate overnight, and then supplemented with MVL5-EVs loaded with GL2 + GL3 siRNA (1.3 μg MVL5/10^9 particles/20nM, 40nM, or 80nM siRNA/well) and incubated for 4 h at 37 °C. Then, cells were washed and cultured in complete media for 24 h. Free siRNA, or mixture siRNA with EVs, or MVL5-EVs without siRNA, or mixture of siRNA and MVL5, or Ambion #1 (negative control #1) at the same concentrations were used as controls. Free media was also used as control. Then, the cells were washed 3x times with PBS, and supplemented with full DMEM media for another 24 h at 37 °C. The cells were lysed at 4 °C in a shaker, and the levels of luminescence were measured as described above.

Statistical analysis

For the all experiments, data are presented as the mean ± S.E.M. Tests for significant differences between the groups were performed using a t-test or one-way ANOVA with multiple comparisons (Fisher's pairwise comparisons) using GraphPad Prism 5.0 (GraphPad software, San Diego, CA, USA). A minimum p value of 0.05 was chosen as the significance level.

Data availability

All data generated or analyzed during this study are included in this published article and its supplementary information file.

Received: 3 May 2024; Accepted: 9 October 2024
Published online: 28 October 2024

References

1. Saraiva, C. et al. Nanoparticle-mediated brain drug delivery: overcoming blood–brain barrier to treat neurodegenerative diseases. *J. Control Release*. **235**, 34–47 (2016).
2. Zhang, Q. et al. Stimuli-responsive gene delivery nanocarriers for cancer therapy. *Nano-Micro Lett.* **15**, 44 (2023).
3. Movahedi, F., Hu, R. G., Becker, D. L. & Xu, C. Stimuli-responsive liposomes for the delivery of nucleic acid therapeutics. *Nanomed. Nanotechnol. Biol. Med.* **11**, 1575–1584 (2015).

4. Dirisala, A. et al. Effective mRNA protection by poly (l-ornithine) synergizes with endosomal escape functionality of a charge-conversion polymer toward maximizing mRNA introduction efficiency. *Macromol. Rapid Commun.* **43**, 2100754 (2022).
5. Lopukhov, A. V. et al. Mannosylated cationic copolymers for gene delivery to macrophages. *Macromol. Biosci.* **21**, 2000371 (2021).
6. Yang, J., Luly, K. M. & Green, J. J. Nonviral nanoparticle gene delivery into the CNS for neurological disorders and brain cancer applications. *Wiley Interdiscip. Rev.: Nanomed. Nanobiotechnol.* **15**, e1853 (2023).
7. Peng, Q. et al. Preformed albumin corona, a protective coating for nanoparticles based drug delivery system. *Biomaterials* **34**, 8521–8530 (2013).
8. Mun, E. A. & Zhaisanbayeva, B. A. The role of nanoparticle PEGylation in drug delivery. *Adv. Mater. Technol.* **2**, 10–18 (2020).
9. Yoshida, K., Burton, G. F., McKinney, J. S., Young, H. & Ellis, E. F. Brain and tissue distribution of polyethylene glycol-conjugated superoxide dismutase in rats. *Stroke* **23**, 865–869 (1992).
10. Veronese, F. M., Caliceti, P., Schiavon, O. & Sergi, M. Polyethylene glycol–superoxide dismutase, a conjugate in search of exploitation. *Adv. Drug Delivery Rev.* **54**, 587–606 (2002).
11. Ibrahim, M. et al. Polyethylene glycol (PEG): the nature, immunogenicity, and role in the hypersensitivity of PEGylated products. *J. Control. Release* **351**, 215–230 (2022).
12. Dams, E. T. et al. Accelerated blood clearance and altered biodistribution of repeated injections of sterically stabilized liposomes. *J. Pharmacol. Exp. Ther.* **292**, 1071–1079 (2000).
13. Ishida, T. et al. Accelerated clearance of a second injection of PEGylated liposomes in mice. *Int. J. Pharm.* **255**, 167–174 (2003).
14. Ishida, T., Kashima, S. & Kiwada, H. The contribution of phagocytic activity of liver macrophages to the accelerated blood clearance (ABC) phenomenon of PEGylated liposomes in rats. *J. Controll. Release* **126**, 162–165 (2008).
15. Hoang Thi, T. T., Pilkington, E. H., Nguyen, D. H., Lee, J. S. & Park, K. D. Truong, N. P. The importance of poly (ethylene glycol) alternatives for overcoming PEG immunogenicity in drug delivery and bioconjugation. *Polymers* **12**, 298 (2020).
16. Farhat, S. C. et al. Air pollution in autoimmune rheumatic diseases: a review. *Autoimmun. Rev.* **11**, 14–21 (2011).
17. Mohamed, B. M. et al. Citrullination of proteins: a common post-translational modification pathway induced by different nanoparticles in vitro and in vivo. *Nanomedicine* **7**, 1181–1195 (2012).
18. Belhadj, Z., Qie, Y., Carney, R., Li, Y. & Nie, G. Current advances in non-viral gene delivery systems: liposomes versus extracellular vesicles. *BMEMat* **1**, e12018 (2023).
19. Théry, C., Amigorena, S., Raposo, G. & Clayton, A. Isolation and characterization of exosomes from cell culture supernatants and biological fluids. *Curr. Protoc. Cell. Biol.* **30**, 3–22 (2006).
20. Théry, C., Ostrowski, M. & Segura, E. Membrane vesicles as conveyors of immune responses. *Nat. Rev. Immunol.* **9**, 581–593 (2009).
21. van den Boorn, J. G., Daßler, J., Coch, C., Schlee, M. & Hartmann, G. Exosomes as nucleic acid nanocarriers. *Adv. Drug Delivery Rev.* **65**, 331–335 (2013).
22. Van Dongen, H. M., Masoumi, N., Witwer, K. W. & Pegtel, D. M. Extracellular vesicles exploit viral entry routes for cargo delivery. *Microbiol. Mol. Biol. Rev.* **80**, 369–386 (2016).
23. Clayton, A., Harris, C. L., Court, J., Mason, M. D. & Morgan, B. P. Antigen-presenting cell exosomes are protected from complement-mediated lysis by expression of CD55 and CD59. *Eur. J. Immunol.* **33**, 522–531 (2003).
24. Kamerkar, S. et al. Exosomes facilitate therapeutic targeting of oncogenic KRAS in pancreatic cancer. *Nature* **546**, 498–503 (2017).
25. Mathieu, M., Martin-Jaular, L., Lavieu, G. & Théry, C. Specificities of secretion and uptake of exosomes and other extracellular vesicles for cell-to-cell communication. *Nat. Cell. Biol.* **21**, 9–17 (2019).
26. Reshke, R. et al. Reduction of the therapeutic dose of silencing RNA by packaging it in extracellular vesicles via a pre-microRNA backbone. *Nat. Biomed. Eng.* **4**, 52–68 (2020).
27. Wang, T. et al. Exosome-based drug delivery systems in cancer therapy. *Chin. Chem. Lett.* **34**, 107508 (2023).
28. Zeng, W., Wen, Z., Chen, H. & Duan, Y. Exosomes as carriers for drug delivery in cancer therapy. *Pharm. Res.* **40**, 873–887 (2023).
29. Wolff, A. C. et al. Recommendations for human epidermal growth factor receptor 2 testing in breast cancer: American Society of Clinical Oncology/College of American Pathologists clinical practice guideline update. *Arch. Pathol. Lab. Med.* **138**, 241–256 (2014).
30. Dent, R. et al. Triple-negative breast cancer: clinical features and patterns of recurrence. *Clin. Cancer Res.* **13**, 4429–4434 (2007).
31. Yu, T. & Di, G. Role of tumor microenvironment in triple-negative breast cancer and its prognostic significance. *Chin. J. Cancer Res.* **29**, 237 (2017).
32. Kim, M. S. et al. Development of exosome-encapsulated paclitaxel to overcome MDR in cancer cells. *Nanomed. Nanotechnol. Biol. Med.* **12**, 655–664 (2016).
33. Haney, M. J. et al. Blood-borne macrophage–neural cell interactions hitchhike on endosome networks for cell-based nanozyme brain delivery. *Nanomedicine* **7**, 815–833 (2012).
34. Haney, M. J. et al. Exosomes as drug delivery vehicles for Parkinson's disease therapy. *J. Control. Release* **207**, 18–30 (2015).
35. Batrakova, E. V. & Kim, M. S. Using exosomes, naturally-equipped nanocarriers, for drug delivery. *J. Control. Release* **219**, 396–405 (2015).
36. Yuan, D. et al. Macrophage exosomes as natural nanocarriers for protein delivery to inflamed brain. *Biomaterials* **142**, 1–12 (2017).
37. Kim, M. S. et al. Engineering macrophage-derived exosomes for targeted paclitaxel delivery to pulmonary metastases: in vitro and in vivo evaluations. *Nanomed. Nanotechnol. Biol. Med.* **14**, 195–204 (2018).
38. Klyachko, N. L., Arzt, C. J., Li, S. M., Gololobova, O. A. & Batrakova, E. V. Extracellular vesicle-based therapeutics: preclinical and clinical investigations. *Pharmaceutics* **12**, 1171 (2020).
39. Zhao, Y. et al. Using extracellular vesicles released by GDNF-Transfected macrophages for therapy of Parkinson disease. *Cells* **11**, 1933 (2022).
40. Kim, S. K., Foote, M. B. & Huang, L. The targeted intracellular delivery of cytochrome C protein to tumors using lipid-apolipoprotein nanoparticles. *Biomaterials* **33**, 3959–3966 (2012).
41. Banks, W. A., Niehoff, M. L., Ponzio, N. M., Erickson, M. A. & Zalcman, S. S. Pharmacokinetics and modeling of immune cell trafficking: quantifying differential influences of target tissues versus lymphocytes in SJL and lipopolysaccharide-treated mice. *J. Neuroinflammation*. **9**, 1–14 (2012).
42. Meyer, O. et al. Cationic liposomes coated with polyethylene glycol as carriers for oligonucleotides. *J. Biol. Chem.* **273**, 15621–15627 (1998).
43. Floch, V. et al. Systemic administration of cationic phosphonolipids/DNA complexes and the relationship between formulation and lung transfection efficiency. *Biochim. et Biophys. Acta (BBA)-Biomembr.* **1464**, 95–103 (2000).
44. Densmore, C. L., Giddings, T. H., Waldrep, J. C., Kinsey, B. M. & Knight, V. Gene transfer by guanidinium-cholesterol: dioleoylphosphatidyl-EtOHamine liposome-DNA complexes in aerosol. *J. Gene. Med.* **1**, 251–264 (1999).
45. Pellegrino, M. et al. Exploiting novel tailored immunotherapies of type 1 diabetes: short interfering RNA delivered by cationic liposomes enables efficient down-regulation of variant PTPN22 gene in T lymphocytes. *Nanomed. Nanotechnol. Biol. Med.* **18**, 371–379 (2019).
46. Pozzi, D., & Caracciolo, G. . Looking back, moving forward: lipid nanoparticles as a promising frontier in gene delivery. *ACS Pharmacol. Transl Sci.* **6**, 1561–1573 (2023).

Acknowledgements
This study was supported in part by the Eshelman Institute for Innovation grant UNC EII 29202 (MH), Russian Science Foundation grant 22-13-00261 (NLK), the State Registration Theme 121041500039-8 and 123032300028-0 (NLK, AVL, IML-D). The part of the equipment used was purchased within the framework of the Lomonosov Moscow University Development Program. Authors are grateful to Professor Alexander V. Kabanov and Professor Elena V. Batrakova for very helpful and fruitful discussion.

Author contributions
Author contributions: Conceptualization, N.K. and E.B.; Methodology, A.L., M.H., N.K., I.Le-D.; Validation, A.L., M.H., N.K., I.Le-D.; Investigation, M.H., N.K.; Writing-original draft preparation, N.K., E.B.; Writing-review and editing, A.L., M.H., N.K., I.Le-D.; Supervision, N.K.; All authors reviewed the manuscript.

Declarations

Competing interests
The authors declare no competing interests.

Additional information
Supplementary Information The online version contains supplementary material available at https://doi.org/10.1038/s41598-024-75985-y.

Correspondence and requests for materials should be addressed to N.L.K.

Reprints and permissions information is available at www.nature.com/reprints.

Publisher's note Springer Nature remains neutral with regard to jurisdictional claims in published maps and institutional affiliations.